

Modern ocean island basalt–like ^{182}W signature in Paleoarchean mafic rocks: Implications for the generation, preservation, and destruction of early mantle heterogeneities

Qing-Feng Mei¹, Jin-Hui Yang^{1,2,*}, Chao-Feng Li¹, Xuan-Ce Wang³, Jukka Konnunaho⁴, Ya-Dong Wu¹, Hong Zhong⁵, Yi-Gang Xu⁶, and Hao Wang¹

¹State Key Laboratory of Lithospheric Evolution, Institute of Geology and Geophysics, Chinese Academy of Sciences, Beijing 100029, China

²College of Earth and Planetary Sciences, University of Chinese Academy of Sciences, Beijing 100049, China

³School of Earth Sciences, Yunnan University, Kunming 650500, China

⁴Geological Survey of Finland, P.O. Box 77, 96101 Rovaniemi, Finland

⁵State Key Laboratory of Ore Deposit Geochemistry, Institute of Geochemistry, Chinese Academy of Sciences, Guiyang 550002, China

⁶State Key Laboratory of Isotope Geochemistry, Guangzhou Institute of Geochemistry, Chinese Academy of Sciences, Guangzhou 510640, China

ABSTRACT

Komatiites and picrites generated by high degrees of mantle partial melting serve as potential probes of Earth's deep mantle. Tungsten (W) isotopes in these rocks offer a rare chance to better understand early differentiation, late accretion, core-mantle interaction, and subsequent evolution of Earth's mantle. We present new W isotope data for Archean komatiites and basalts from the Barberton (South Africa) and Suomussalmi (Finland) Greenstone Belts and Permian picrites from the Emeishan large igneous province (China). The Paleoarchean samples from the Barberton Greenstone Belt have modern ocean island basalt (OIB)–like $\mu^{182}\text{W}$ values ranging from -20.4 to $+5.6$, whereas the Mesoarchean komatiites from the Suomussalmi Greenstone Belt show $\mu^{182}\text{W}$ values of -2.2 to $+11.3$. The Permian Emeishan picrites give $\mu^{182}\text{W}$ values of -7.1 to $+3.1$. Our data, combined with the published global data set, show that W isotope heterogeneity in the mantle has existed throughout Earth's history, with positive $\mu^{182}\text{W}$ values transitioning to near-zero in the upper mantle by the end of the Archean. The negative $\mu^{182}\text{W}$ values of Paleoarchean samples in the Barberton Greenstone Belt and modern OIBs likely result from either early differentiation or core-mantle interaction. The incorporation of a plume-delivered negative $\mu^{182}\text{W}$ component and enhanced mantle mixing is a viable mechanism to explain the transition of $\mu^{182}\text{W}$ values in the upper mantle from positive to near-zero, while recycling of crustal materials into the mantle would result in a shift of negative $\mu^{182}\text{W}$ values of the lower mantle closer to zero since the onset of plate tectonics. The latter process could possibly explain the slightly negative to near-zero $\mu^{182}\text{W}$ values of the Emeishan picrites and some kimberlites. The well-resolved negative $\mu^{182}\text{W}$ anomalies observed in this study provide important insights into the generation, preservation, and obliteration of W isotope heterogeneities in the lower mantle.


INTRODUCTION

Chemical heterogeneities in the terrestrial mantle have long been identified, and some of them have been proposed to have been generated early in Earth's history, by studies that

investigated short-lived isotope systematics (e.g., ^{129}I – ^{129}Xe , ^{146}Sm – ^{142}Nd , and ^{182}Hf – ^{182}W ; Willbold et al., 2011; Mukhopadhyay, 2012; Touboul et al., 2012; Peters et al., 2018; Puchtel et al., 2022). Archean mantle-derived rocks show a wide range of isotopic tungsten ($\mu^{182}\text{W}$) values (-11.4 to $+23.4$), where the μ value represents the deviation of measured isotope ratio, in parts per million, from laboratory standards (e.g.,

Puchtel et al., 2022). These W isotopic heterogeneities are interpreted as the result of either early differentiation that occurred within the lifetime of ^{182}Hf or an initially uneven distribution of late accreted materials (grainy late accretion) in the ancient mantle and provide important constraints on Earth's geodynamic evolution (e.g., Willbold et al., 2011; Touboul et al., 2012; Puchtel et al., 2016a, 2022; Tusch et al., 2022).

Recent studies suggest that positive $\mu^{182}\text{W}$ anomalies in the upper mantle dissipated by the end of the Archean (Mei et al., 2020; Tusch et al., 2021; Nakanishi et al., 2023). During Earth's core formation (within the lifetime of ^{182}Hf), Hf was completely partitioned into the mantle because it is a strongly lithophile element. The core, therefore, became highly depleted in ^{182}W relative to the mantle because no radiogenic ^{182}W accumulated in the core after the metal-silicate segregation. Mass balance calculations imply that the core has a strongly negative $\mu^{182}\text{W}$ value of ~ -220 (e.g., Kleine et al., 2009; Touboul et al., 2012). Thus, core-mantle interaction offers a plausible cause for the decrease in $\mu^{182}\text{W}$ during the Archean and the ^{182}W deficits observed in the Phanerozoic ocean island basalts (OIBs) (e.g., Rizo et al., 2019; Mundl-Petermeier et al., 2020; Peters et al., 2021). Tungsten isotopes of the plume-derived samples (i.e., komatiite, picrite, and OIBs formed at different periods) have the potential to reveal the nature of the deep mantle and to trace core-mantle interaction through-

Jin-Hui Yang  <https://orcid.org/0000-0001-8373-0620>
*jinhui@mail.igcas.ac.cn

CITATION: Mei, Q.-F., et al., 2023, Modern ocean island basalt–like ^{182}W signature in Paleoarchean mafic rocks: Implications for the generation, preservation, and destruction of early mantle heterogeneities: *Geology*, v. 51, p. 919–923, <https://doi.org/10.1130/G51354.1>

out Earth's history. We report high-precision W isotope data for the Archean komatiites and basalts from the Barberton Granitoid–Greenstone Terrane (BGGT, southern Africa) and the Suomussalmi Greenstone Belt (SGB, Finland) as well as Permian picrites from the Emeishan large igneous province (Emeishan LIP, China) to better understand the mechanisms for creating early mantle heterogeneities and possible core-mantle interaction throughout Earth's history. High-precision ^{142}Nd isotope analyses were performed for those samples showing W isotopic anomalies to evaluate the influence of early mantle differentiation processes.

SAMPLES AND ANALYTICAL RESULTS

The BGGT komatiites and basalts are from the Kromberg (ca. 3.33 Ga) and Theespruit (ca. 3.53 Ga) Formations, Onverwacht Group (Lowe and Byerly, 2007) (Fig. 1A). A 3.28 Ga

granodiorite was collected from the Ngwane gneiss suite, Ancient Gneiss Complex (AGC) (Kröner et al., 2019). The SGB (2.94–2.82 Ga) komatiite samples were from drill cores of the Hietahrju Ni-Cu-Co-PGE deposit (Konnunaho et al., 2016; Lehtonen et al., 2017) (Fig. 1B). The picrites of the ca. 0.26 Ga Emeishan LIP were collected from Lijiang and Dali areas (Zhong et al., 2014) (Fig. 1C). Detailed information on the geological background is provided in the Supplemental Material¹.

Major and trace element concentrations and W-Nd isotope compositions of the samples were measured at the Institute of Geology and

Geophysics, Chinese Academy of Sciences (Beijing). Tungsten and Nd isotope measurements were conducted using the Thermo Fisher Neptune multicollector–inductively coupled plasma–mass spectrometer (MC-ICP-MS) and Triton Plus thermal ionization mass spectrometer (TIMS), respectively. The detailed procedures are described in the Supplemental Material. The external reproducibility of $\mu^{182}\text{W}$ for standard solution Alfa Aesar W in this study is ± 6.1 . The external reproducibility of $\mu^{142}\text{Nd}$ for standard solution JNdi-1 is ± 4.8 (Li et al., 2015).

Measured $\mu^{182}\text{W}$ and $\mu^{183}\text{W}$ values of the samples are shown in Figure 2. The basalt sample (15SA07) from the Theespruit Formation displays similar $\mu^{182}\text{W}$ and $\mu^{183}\text{W}$ relative to the standard. The basalt sample from the Kromberg Formation (15SA22) has $\mu^{182}\text{W}$ values of -20.4 ± 6.1 (2 standard errors [SE]) and

¹Supplemental Material. Supplemental information, tables, and figures. Please visit <https://doi.org/10.1130/GEOL.S.23669295> to access the supplemental material, and contact editing@geosociety.org with any questions.

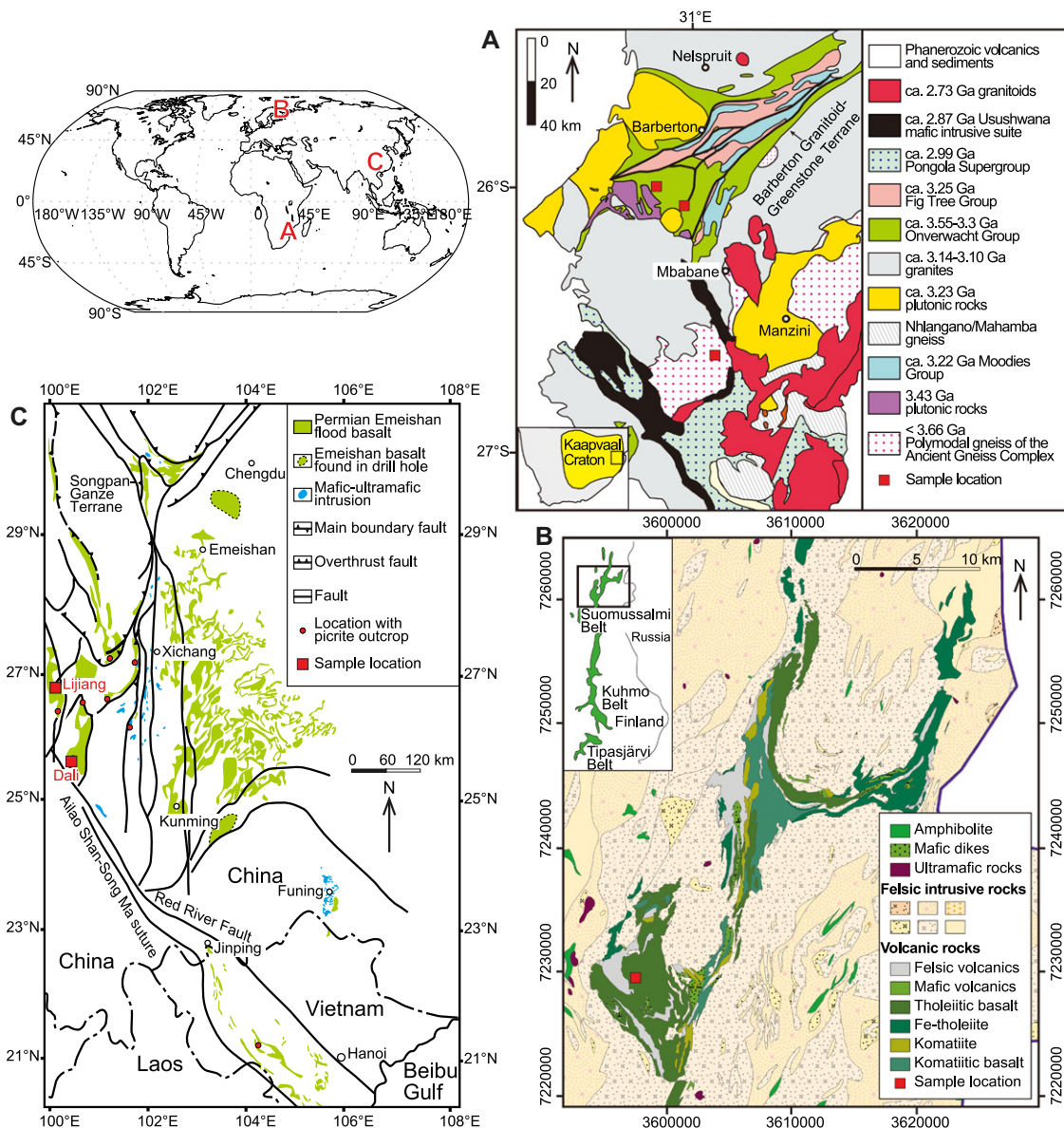


Figure 1. Simplified geologic maps showing sample locations. (A) Ancient Gneiss Complex and Barberton Granitoid–Greenstone Terrane in the eastern Kaapvaal Craton, southern Africa; after Kröner et al. (2019). (B) Suomussalmi Greenstone Belt in Finland (based on DigiKP, the digital map database of the Geological Survey of Finland, available at: <http://www.geo.fi/en/bed-rock.html>). (C) Emeishan large igneous province in China, after Kamenetsky et al. (2012).

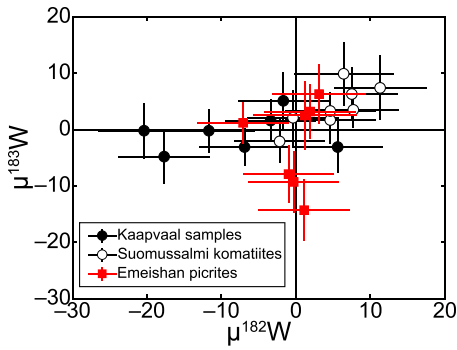


Figure 2. Measured $\mu^{182}\text{W}$ and $\mu^{183}\text{W}$ values for samples of this study. Error bars represent 2 standard errors.

-17.7 ± 6.1 (2SE) for two duplicate dissolution aliquots and $\mu^{183}\text{W}$ values indistinguishable from the standard. Sample 15SA22 has a $\mu^{142}\text{Nd}$ value of $+3.6 \pm 4.6$ (2SE), indistinguishable from the standard. Individual measurements of granodiorite sample SA31 from the AGC also gave negative $\mu^{182}\text{W}$ values of -6.9 ± 6.1 (2SE) and -11.7 ± 6.1 (2SE), $\mu^{183}\text{W}$ values close to 0, and a $\mu^{142}\text{Nd}$ value of 0.0 ± 4.5 (2SE). The drill core samples from the SGB show $\mu^{182}\text{W}$ values of -2.2 to $+11.3$ and $\mu^{183}\text{W}$ values of -2.1 to $+9.9$. Emeishan picrites exhibit no well-resolved $\mu^{182}\text{W}$ anomaly but a wide range of $\mu^{183}\text{W}$ values varying from -14.3 to $+6.3$. Sample DJ-0803 from Lijiang has the lowest $\mu^{182}\text{W}$ value (-7.1 ± 6.1 , 2SE) among the analyzed Emeishan picrites. The negative $\mu^{183}\text{W}$ anomalies in Emeishan picrites likely indicate the mass-independent isotope fractionation caused by magnetic isotope effect (Budde et al., 2022), which has negligible effects on the measured $\mu^{182}\text{W}$ values that are calculated from isotopic ratios normalized to $^{186}\text{W}/^{184}\text{W} = 0.92767$. Data for all samples and standards are provided in the Supplemental Material.

DISCUSSION AND CONCLUSION

The BGGT and SGB samples have experienced greenschist- to amphibolite-facies metamorphism (Lowe and Byerly, 2007; Konnunaho et al., 2016) and have high W/Th ratios (0.82–1.77), indicating a possible fluid-induced W enrichment in these samples. However, the negative correlation between $\mu^{182}\text{W}$ and $\epsilon^{143}\text{Nd}(t)$ of the BGGT samples indicates that their W isotopic compositions have not been affected by post-magmatic processes, as suggested by Tusch et al. (2022) and our data (see the Supplemental Material). The Permian Emeishan picrites have near-canonical W/Th ratios of 0.06–0.17, reflecting undisturbed elemental W systematics.

Our new results and the published global data set for mantle-derived rocks are shown in Figure 3. It shows that Eoarchean rocks commonly have positive $\mu^{182}\text{W}$ values averaging $\sim +13$ (Tusch et al., 2021). Most Paleoproterozoic

to Neoproterozoic samples have either positive or near-zero $\mu^{182}\text{W}$ values except for some samples from the Kaapvaal Craton (i.e., Schapenburg Greenstone Remnant, BGGT, and AGC) that exhibit resolvable negative $\mu^{182}\text{W}$ values (Puchtel et al., 2016a; Tusch et al., 2022). Tusch et al. (2022) first observed a negative covariation of $\mu^{182}\text{W}$ with $\epsilon^{143}\text{Nd}(t)$ and $\epsilon^{176}\text{Hf}(t)$ for mantle-derived rocks in the Kaapvaal Craton, and proposed a geodynamic model involving early silicate differentiation and recycling of lower crustal restites that remained after partial melting of a Hadean protocrust, in order to explain the ^{182}W - ^{142}Nd - ^{143}Nd - ^{176}Hf isotope compositions of these rocks. Notably, our new W-Nd isotope data for samples from the Kromberg and Theespruit Formations are consistent with the covariation (Fig. 4A). The sample with the most negative $\mu^{182}\text{W}$ value among the Kaapvaal rocks shows a near-zero $\mu^{142}\text{Nd}$ value, possibly indicating a two-stage differentiation model; i.e., the first differentiation occurred within the lifetime of ^{182}Hf and the second differentiation occurred while ^{146}Sm was still extant but ^{182}Hf was extinct (Fig. 4B). This is consistent with the two-stage process proposed by Tusch et al. (2022); i.e., formation of a mafic protocrust by ca. 50 Ma after solar system formation and partial protocrustal anatexis between ca. 4.35 and 4.25 Ga.

Apart from early differentiation within the lifetime of ^{182}Hf , a sluggish mixing of late accreted materials and core-mantle interaction provide alternative explanations for the negative $\mu^{182}\text{W}$ anomalies in the mantle-derived rocks due to strongly negative $\mu^{182}\text{W}$ values of chondrites (~ -190) and Earth's core (~ -220) (Kleine et al., 2009; Willbold et al., 2011; Rizo et al., 2019; Mundl-Petermeier et al., 2020; Nakanishi et al., 2021). However, the 3.46 Ga Dwalile komatiite suite from the AGC has modern mantle-like Ru isotope composition, distinct from coupled ^{100}Ru - ^{102}Ru deficits of late accreted materials, arguing against the explanation that the ^{182}W deficits in the Kaapvaal Craton originated from an excess of late accreted materials (Fischer-Gödde et al., 2020; Tusch et al., 2022). Another potential reservoir with negative $\mu^{182}\text{W}$ anomalies is Earth's core. However, direct physical input of core metal into plumes can be ruled out due to the absence of highly siderophile element enrichments in OIBs. Possible mechanisms for core-mantle interaction include Si-Mg-Fe oxide exsolutions and isotopic core-mantle equilibration (Rizo et al., 2019; Mundl-Petermeier et al., 2020). Conceptually, these core-mantle interaction mechanisms can explain negative $\mu^{182}\text{W}$ signatures in the source of samples from the Kaapvaal Craton.

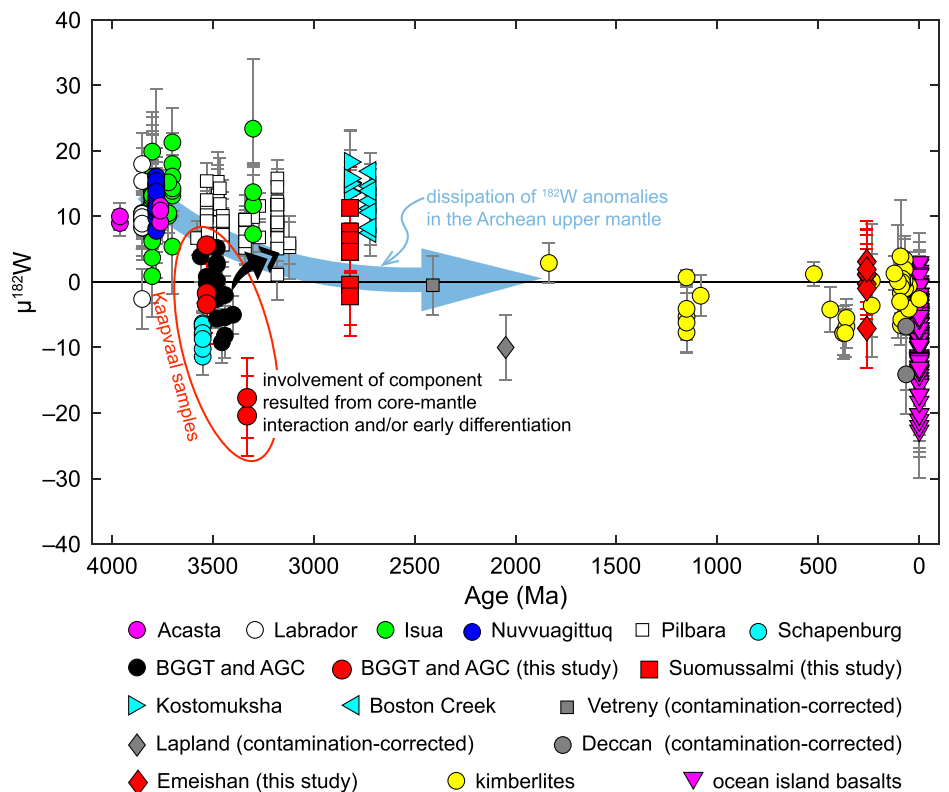


Figure 3. Compilation of the $\mu^{182}\text{W}$ values for the mantle-derived rocks. Error bars represent 2 standard errors. References and information about the data, including geographic locations, are provided in Table S5 in the Supplemental Material (see text footnote 1). The large blue arrow indicates the dissipation of ^{182}W anomalies in the Archean upper mantle (Mei et al., 2020; Nakanishi et al., 2023).

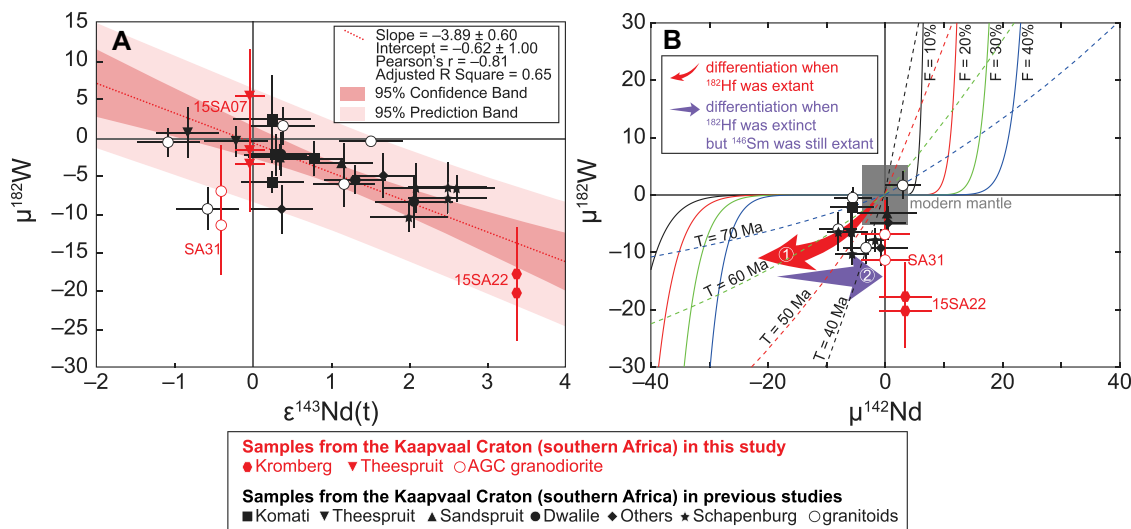


Figure 4. Measured $\mu^{182}\text{W}$ versus $\epsilon^{143}\text{Nd}(t)$ (A) and $\mu^{142}\text{Nd}$ (B) for samples from the Kaapvaal Craton (southern Africa), including data from the literature (black marker edge) and this study (red marker edge). Error bars represent 2 standard errors. The red dotted line in A showing the correlation of $\mu^{182}\text{W}$ with $\epsilon^{143}\text{Nd}(t)$ values is the best-fit regression through the data of mantle-derived samples (black and red filled symbols) with the 95% confidence and prediction bands. This correlation was referred to as the Kaapvaal mantle array and first observed by Tusch et al. (2022). The

solid curves in B correspond to modeled W-Nd isotope composition for products of different melting degree (F) from a modern mantle source. The dashed curves indicate loci of identical T (time interval between the solar system formation and the early silicate differentiation) for the formation of these reservoirs. Details of this model, as well as geographic locations, are provided in the Supplemental Material (see text footnote 1). Data of the Komati and Schapenburg komatiites are from Touboul et al. (2012), Puchtel et al. (2013), and Puchtel et al. (2016a). Other literature data are from Tusch et al. (2022). AGC—Ancient Gneiss Complex.

Previous studies on Proterozoic mantle-derived samples reported near-zero to negative $\mu^{182}\text{W}$ values for the 2.41 Ga and 2.05 Ga komatiitic basalts (Vetreny and Lapland) and kimberlites (Tanzania and South Africa) (Fig. 3; Puchtel et al., 2016b, 2020; Tappe et al., 2020; Nakanishi et al., 2021). Recently reported W isotopes of granites and schists with ancient Nd model ages (from ca. 3.6 Ga to 2.3 Ga) further strengthen the transition of $\mu^{182}\text{W}$ values in the upper mantle from averaging +13 at the Eoarchean to near-zero at the early Proterozoic (Nakanishi et al., 2023). This transition may be caused by efficient mixing of the unhomogenized late-accreted components (Puchtel et al., 2022) and/or by addition of plume materials with negative $\mu^{182}\text{W}$ (e.g., the source of the measured Kaapvaal samples) (Peters et al., 2021). A similar disappearance of resolvable positive and negative ^{142}Nd anomalies in the mafic-ultramafic rock record during the transition period (from 3.6 to 2.4 Ga) has also been observed (e.g., Schneider et al., 2018; Puchtel et al., 2022). These transitions indicate that the primordial ^{182}W - ^{142}Nd isotopic heterogeneities in the upper mantle had been largely destroyed through vigorous convective mantle mixing by the beginning of the Proterozoic (Mei et al., 2020; Puchtel et al., 2022; Nakanishi et al., 2023).

Phanerozoic OIBs, kimberlites, and samples from the Deccan Traps and Emeishan LIP have a wide range of $\mu^{182}\text{W}$ values, from near-zero to negative values as low as -23 (Rizo et al., 2019; Mundl-Petermeier et al., 2020; Tappe et al., 2020; Nakanishi et al., 2021; Peters et al., 2021) (Fig. 3). Jackson et al. (2020) revealed that the most negative $\mu^{182}\text{W}$ anomalies were exclusively observed in the OIB samples with

high $^{143}\text{Nd}/^{144}\text{Nd}$ ratios and low $^{206}\text{Pb}/^{204}\text{Pb}$ ratios, while the OIBs without anomalous ^{182}W compositions were derived from a mantle source that had been added by recycled materials. The characteristics of Sr-Nd-Pb and W isotopes for OIBs suggest that recycled crustal materials may result in a shift of $\mu^{182}\text{W}$ values closer to zero (Jackson et al., 2020). Our results show that the Dali picrites have no $\mu^{182}\text{W}$ anomalies, while one of the Lijiang picrites has a negative $\mu^{182}\text{W}$ value of -7.1 ± 6.1 (2SE). Previous Sr-Nd-Pb isotopic studies on melt inclusions and whole rock demonstrate that more recycled crustal materials had been involved in the source of Dali picrites than that of Lijiang picrites (Zhang et al., 2006; Hanski et al., 2010; Ren et al., 2017; Zhang et al., 2019; Zhang et al., 2021). Therefore, we consider it most likely that the W isotope composition of the Emeishan picrites was influenced by recycled materials in their mantle sources, similar to OIBs (Jackson et al., 2020).

Collectively, the global data set for terrestrial rocks reveals W isotopic heterogeneities in the Archean mantle, likely resulting from early silicate differentiation, grainy late accretion, or core-mantle interaction (Willbold et al., 2011; Touboul et al., 2012; Rizo et al., 2019; Mundl-Petermeier et al., 2020). Notably, our Paleoarchean Kromberg sample has a $\mu^{182}\text{W}$ value of -19.1 ± 4.3 (2SE), identical to the most-negative $\mu^{182}\text{W}$ value observed in modern OIBs (-22.7 ± 3.3 , 2SE; Mundl-Petermeier et al., 2020). The W isotopic heterogeneities in the upper mantle had been largely eliminated by the end of the Archean (Mei et al., 2020; Tusch et al., 2021; Nakanishi et al., 2023). Moreover, Phanerozoic plume-derived rocks (e.g., Emeishan picrites in this study) have $\mu^{182}\text{W}$ values

ranging from negative to zero. These indicate that recycling of crustal materials and mantle mixing would have partially homogenized W isotopes in the lower mantle since the onset of plate tectonics on Earth.

ACKNOWLEDGMENTS

We thank Han Zhao, Lei Yang, and the technical staff at the MC-ICP-MS laboratory of the Institute of Geology and Geophysics, Chinese Academy of Sciences, for their valuable assistance, as well as Yining Zhang for insightful discussions. We also appreciate the editorial support of Urs Schaltegger and careful reviews by Jingao Liu, Jonas Tusch, Bradley Peters, and two anonymous reviewers for their helpful comments. This research was supported by the National Natural Science Foundation of China (grants 42103011 and 42003029).

REFERENCES CITED

- Budde, G., Archer, G.J., Tissot, F.L.H., Tappe, S., and Kleine, T., 2022, Origin of the analytical ^{183}W effect and its implications for tungsten isotope analyses: *Journal of Analytical Atomic Spectrometry*, v. 37, p. 2005–2021, <https://doi.org/10.1039/D2JA00102K>.
- Fischer-Gödde, M., Elfers, B.M., Münker, C., Szilas, K., Maier, W.D., Messling, N., Morishita, T., Van Kranendonk, M., and Smithies, H., 2020, Ruthenium isotope vestige of Earth's pre-late-veener mantle preserved in Archean rocks: *Nature*, v. 579, p. 240–244, <https://doi.org/10.1038/s41586-020-2069-3>.
- Hanski, E., Kamenetsky, V.S., Luo, Z.Y., Xu, Y.G., and Kuzmin, D.V., 2010, Primitive magmas in the Emeishan large igneous province, southwestern China and northern Vietnam: *Lithos*, v. 119, p. 75–90, <https://doi.org/10.1016/j.lithos.2010.04.008>.
- Jackson, M.G., et al., 2020, Ancient helium and tungsten isotopic signatures preserved in mantle domains least modified by crustal recycling: *Proceedings of the National Academy of Sciences of the United States of America*, v. 117, p. 30,993–31,001, <https://doi.org/10.1073/pnas.2009663117>.

- Kamenetsky, V.S., Chung, S.L., Kamenetsky, M.B., and Kuzmin, D.V., 2012, Picrites from the Emeishan Large Igneous Province, SW China: A compositional continuum in primitive magmas and their respective mantle sources: *Journal of Petrology*, v. 53, p. 2095–2113, <https://doi.org/10.1093/petrology/egs045>.
- Kleine, T., Touboul, M., Bourdon, B., Nimmo, F., Mezger, K., Palme, H., Jacobsen, S.B., Yin, Q.-Z., and Halliday, A.N., 2009, Hf–W chronology of the accretion and early evolution of asteroids and terrestrial planets: *Geochimica et Cosmochimica Acta*, v. 73, p. 5150–5188, <https://doi.org/10.1016/j.gca.2008.11.047>.
- Konnunaho, J., Hanski, E., Wing, B., Bekker, A., Lukkari, S., and Halkoaho, T., 2016, The Hietaharju PGE-enriched komatiite-hosted sulfide deposit in the Archean Suomussalmi greenstone belt, eastern Finland: *Ore Geology Reviews*, v. 72, p. 641–658, <https://doi.org/10.1016/j.oregeorev.2015.08.022>.
- Kröner, A., Hoffmann, J.E., Wong, J.M., Geng, H.-Y., Schneider, K.P., Xie, H., Yang, J.-H., and Nhkoko, N., 2019, Archean crystalline rocks of the Eastern Kaapvaal Craton, in Kröner, A., and Hofmann, A., eds., *The Archean Geology of the Kaapvaal Craton, Southern Africa*: Cham, Springer, p. 1–32, https://doi.org/10.1007/978-3-319-78652-0_1.
- Lehtonen, E., Heilimo, E., Halkoaho, T., Hölttä, P., and Huhma, H., 2017, The temporal variation of Mesoproterozoic volcanism in the Suomussalmi greenstone belt, Karelia Province, Eastern Finland: *International Journal of Earth Sciences*, v. 106, p. 763–781, <https://doi.org/10.1007/s00531-016-1327-y>; erratum available at <https://doi.org/10.1007/s00531-016-1348-6>.
- Li, C.-F., Wang, X.-C., Li, Y.-L., Chu, Z.-Y., Guo, J.-H., and Li, X.-H., 2015, Ce–Nd separation by solid-phase micro-extraction and its application to high-precision $^{142}\text{Nd}/^{144}\text{Nd}$ measurements using TIMS in geological materials: *Journal of Analytical Atomic Spectrometry*, v. 30, p. 895–902, <https://doi.org/10.1039/C4JA00328D>.
- Lowe, D.R., and Byerly, G.R., 2007, An overview of the geology of the Barberton Greenstone Belt and vicinity: Implications for early crustal development, in van Kranendonk, M.J., et al., eds., *Developments in Precambrian Geology*: Amsterdam, Elsevier, p. 481–526, [https://doi.org/10.1016/S0166-2635\(07\)15053-2](https://doi.org/10.1016/S0166-2635(07)15053-2).
- Mei, Q.-F., Yang, J.-H., Wang, Y.-F., Wang, H., and Peng, P., 2020, Tungsten isotopic constraints on homogenization of the Archean silicate Earth: Implications for the transition of tectonic regimes: *Geochimica et Cosmochimica Acta*, v. 278, p. 51–64, <https://doi.org/10.1016/j.gca.2019.07.050>.
- Mukhopadhyay, S., 2012, Early differentiation and volatile accretion recorded in deep-mantle neon and xenon: *Nature*, v. 486, p. 101–104, <https://doi.org/10.1038/nature11141>.
- Mundl-Petermeier, A., Walker, R.J., Fischer, R.A., Leric, V., Jackson, M.G., and Kurz, M.D., 2020, Anomalous ^{182}W in high $^3\text{He}/^4\text{He}$ ocean island basalts: Fingerprints of Earth's core?: *Geochimica et Cosmochimica Acta*, v. 271, p. 194–211, <https://doi.org/10.1016/j.gca.2019.12.020>.
- Nakanishi, N., Giuliani, A., Carlson, R.W., Horan, M.F., Woodhead, J., Pearson, D.G., and Walker, R.J., 2021, Tungsten-182 evidence for an ancient kimberlite source: Proceedings of the National Academy of Sciences of the United States of America, v. 118, <https://doi.org/10.1073/pnas.2020680118>.
- Nakanishi, N., Puchtel, I.S., Walker, R.J., and Nabelek, P.I., 2023, Dissipation of tungsten-182 anomalies in the Archean upper mantle: Evidence from the Black Hills, South Dakota, USA: *Chemical Geology*, v. 617, <https://doi.org/10.1016/j.chemgeo.2022.121255>.
- Peters, B.J., Carlson, R.W., Day, J.M.D., and Horan, M.F., 2018, Hadean silicate differentiation preserved by anomalous $^{142}\text{Nd}/^{144}\text{Nd}$ ratios in the Réunion hotspot source: *Nature*, v. 555, p. 89–93, <https://doi.org/10.1038/nature25754>.
- Peters, B.J., Mundl-Petermeier, A., Carlson, R.W., Walker, R.J., and Day, J.M.D., 2021, Combined lithophile-siderophile isotopic constraints on Hadean processes preserved in ocean island basalt sources: *Geochemistry, Geophysics, Geosystems*, v. 22, <https://doi.org/10.1029/2020GC009479>.
- Puchtel, I.S., Blichert-Toft, J., Touboul, M., Walker, R.J., Byerly, G.R., Nisbet, E.G., and Anhaeusser, C.R., 2013, Insights into early Earth from Barberton komatiites: Evidence from lithophile isotope and trace element systematics: *Geochimica et Cosmochimica Acta*, v. 108, p. 63–90, <https://doi.org/10.1016/j.gca.2013.01.016>.
- Puchtel, I.S., Blichert-Toft, J., Touboul, M., Horan, M.F., and Walker, R.J., 2016a, The coupled ^{182}W - ^{142}Nd record of early terrestrial mantle differentiation: *Geochemistry, Geophysics, Geosystems*, v. 17, p. 2168–2193, <https://doi.org/10.1002/2016GC006324>.
- Puchtel, I.S., Touboul, M., Blichert-Toft, J., Walker, R.J., Brandon, A.D., Nicklas, R.W., Kulikov, V.S., and Samsonov, A.V., 2016b, Lithophile and siderophile element systematics of Earth's mantle at the Archean–Proterozoic boundary: Evidence from 2.4 Ga komatiites: *Geochimica et Cosmochimica Acta*, v. 180, p. 227–255, <https://doi.org/10.1016/j.gca.2016.02.027>.
- Puchtel, I.S., Mundl-Petermeier, A., Horan, M., Hanski, E.J., Blichert-Toft, J., and Walker, R.J., 2020, Ultra-depleted 2.05 Ga komatiites of Finnish Lapland: Products of grainy late accretion or core-mantle interaction?: *Chemical Geology*, v. 554, <https://doi.org/10.1016/j.chemgeo.2020.119801>.
- Puchtel, I.S., Blichert-Toft, J., Horan, M.F., Touboul, M., and Walker, R.J., 2022, The komatiite testimony to ancient mantle heterogeneity: *Chemical Geology*, v. 594, <https://doi.org/10.1016/j.chemgeo.2022.120776>.
- Ren, Z.-Y., Wu, Y.-D., Zhang, L., Nichols, A.R.L., Hong, L.-B., Zhang, Y.-H., Zhang, Y., Liu, J.-Q., and Xu, Y.-G., 2017, Primary magmas and mantle sources of Emeishan basalts constrained from major element, trace element and Pb isotope compositions of olivine-hosted melt inclusions: *Geochimica et Cosmochimica Acta*, v. 208, p. 63–85, <https://doi.org/10.1016/j.gca.2017.01.054>.
- Rizo, H., Andraut, D., Bennett, N.R., Humayun, M., Brandon, A., Vlastelic, I., Moine, B., Poirier, A., Bouhifd, M.A., and Murphy, D.T., 2019, ^{182}W evidence for core-mantle interaction in the source of mantle plumes: *Geochemical Perspectives Letters*, v. 11, p. 6–11, <https://doi.org/10.7185/geochemlet.1917>.
- Schneider, K.P., Hoffmann, J.E., Boyet, M., Münker, C., and Kröner, A., 2018, Coexistence of enriched and modern-like ^{142}Nd signatures in Archean igneous rocks of the eastern Kaapvaal Craton, southern Africa: *Earth and Planetary Science Letters*, v. 487, p. 54–66, <https://doi.org/10.1016/j.epsl.2018.01.022>.
- Tappe, S., Budde, G., Stracke, A., Wilson, A., and Kleine, T., 2020, The tungsten-182 record of kimberlites above the African superplume: Exploring links to the core-mantle boundary: *Earth and Planetary Science Letters*, v. 547, <https://doi.org/10.1016/j.epsl.2020.116473>.
- Touboul, M., Puchtel, I.S., and Walker, R.J., 2012, ^{182}W evidence for long-term preservation of early mantle differentiation products: *Science*, v. 335, p. 1065–1069, <https://doi.org/10.1126/science.1216351>.
- Tusch, J., Münker, C., Hasenstab, E., Jansen, M., Marien, C.S., Kurzweil, F., Van Kranendonk, M.J., Smithies, H., Maier, W., and Garbe-Schönberg, D., 2021, Convective isolation of Hadean mantle reservoirs through Archean time: Proceedings of the National Academy of Sciences of the United States of America, v. 118, <https://doi.org/10.1073/pnas.2012626118>.
- Tusch, J., Hoffmann, J.E., Hasenstab, E., Fischer-Gödde, M., Marien, C.S., Wilson, A.H., and Münker, C., 2022, Long-term preservation of Hadean protocrust in Earth's mantle: Proceedings of the National Academy of Sciences of the United States of America, v. 119, <https://doi.org/10.1073/pnas.2120241119>.
- Willbold, M., Elliott, T., and Moorbath, S., 2011, The tungsten isotopic composition of the Earth's mantle before the terminal bombardment: *Nature*, v. 477, p. 195–198, <https://doi.org/10.1038/nature10399>.
- Zhang, L., Ren, Z.Y., Handler, M.R., Wu, Y.D., Zhang, L., Qian, S.P., Xia, X.P., Yang, Q., and Xu, Y.G., 2019, The origins of high-Ti and low-Ti magmas in large igneous provinces, insights from melt inclusion trace elements and Sr–Pb isotopes in the Emeishan large Igneous Province: *Lithos*, v. 344–345, p. 122–133, <https://doi.org/10.1016/j.lithos.2019.06.014>.
- Zhang, L., Ren, Z.Y., Zhang, L., Wu, Y.D., Qian, S.P., Xia, X.P., and Xu, Y.G., 2021, Nature of the mantle plume under the Emeishan large igneous province: Constraints from olivine-hosted melt inclusions of the Lijiang picrites: *Journal of Geophysical Research: Solid Earth*, v. 126, <https://doi.org/10.1029/2020JB021022>.
- Zhang, Z., Mahoney, J.J., Mao, J., and Wang, F., 2006, Geochemistry of picritic and associated basalt flows of the western Emeishan flood basalt province, China: *Journal of Petrology*, v. 47, p. 1997–2019, <https://doi.org/10.1093/petrology/egl034>.
- Zhong, Y.T., He, B., Mundil, R., and Xu, Y.G., 2014, CA-TIMS zircon U–Pb dating of felsic ignimbrite from the Binchuan section: Implications for the termination age of Emeishan large igneous province: *Lithos*, v. 204, p. 14–19, <https://doi.org/10.1016/j.lithos.2014.03.005>.

Printed in the USA